Atmos. Chem. Phys. Discuss., 12, 19987–20006, 2012
www.atmos-chem-phys-discuss.net/12/19987/2012/
doi:10.5194/acpd-12-19987-2012

Atmospheric Chemistry and Physics Discussions

The effects of hygroscopicity of fossil fuel combustion aerosols on mixed-phase clouds

Y. Yun[1], **J. E. Penner**[1], **and O. Popovicheva**[2]

[1]Department of Atmospheric, Oceanic, and Space Sciences, University of Michigan, Ann Arbor, MI 48105, USA
[2]D. V. Skobeltsyn Institute of Nuclear Physics, M. V. Lomonosov Moscow State University, Moscow, 119234, Russia

Received: 8 July 2012 – Accepted: 30 July 2012 – Published: 9 August 2012

Correspondence to: Y. Yun (yuxingy@umich.edu)

Published by Copernicus Publications on behalf of the European Geosciences Union.

Abstract

Fossil fuel black carbon and organic matter (ffBC/OM) are often emitted together with sulfate, which coats the surface of these particles and changes their hygroscopicity. Observational studies show that the hygroscopicity of soot particles can modulate their ice nucleation ability. To address this, we implemented a scheme that uses 3 levels of soot hygroscopicity (hydrophobic, hydrophilic and hygroscopic) and used laboratory data to specify their ice nuclei abilities. The new scheme results in significant changes to anthropogenic forcing in mixed-phase clouds. The net forcing in off-line studies varies from 0.111 to 1.059 $W\,m^{-2}$ depending on the ice nucleation capability of hygroscopic soot particles. The total anthropogenic cloud forcing and whole-sky forcing with the new scheme is 0.06 $W\,m^{-2}$ and $-2.45\,W\,m^{-2}$, respectively, but could be more positive if hygroscopic soot particles are allowed to nucleate ice particles. The change in liquid water path dominates the anthropogenic forcing in mixed-phase clouds.

1 Introduction

Soot aerosols produced by fossil fuel and biomass burning contain both black carbon (BC) and organic matter (OM). Both act to absorb solar radiation, thereby changing vertical temperature profiles and decreasing surface radiation. Combustion aerosols can also act as cloud condensation nuclei, causing indirect effects on clouds by decreasing the cloud droplet radius. This causes cooling which counteracts the warming by greenhouse gases. Combustion aerosols can also act as heterogeneous ice nuclei (IN) in mixed-phase clouds (e.g., Cozic et al., 2008), as well as in cirrus clouds (Koehler et al., 2009; Penner et al., 2009). Their ice effects are much more uncertain, which hinders climate prediction. Due to the abundance of fossil fuel (ff) combustion aerosols, a small change in their ice nucleation ability can produce a large difference in indirect effects. Several studies have noted the sensitivity of aerosol forcing to ice nucleation in

ACPD

12, 19987–20006, 2012

mixed-phase clouds (Lohmann and Hoose, 2009; Storelvmo et al., 2011, 2008a; Yun and Penner, 2012).

During the lifetime of soot aerosols in the atmosphere their hygroscopicity can be altered through coating by sulfate (Zhang et al., 2008). Several laboratory experiments have investigated the effect of coating on the ability of soot particles to nucleate ice (DeMott et al., 1999; Mohler et al., 2005; Friedman et al., 2011; Crawford et al., 2011). DeMott et al. (1999) conducted experiments ice nucleation on lamp black soot at 213–233 K with sulfuric acid coating varying from zero to several weight percent. It was found that ice nucleation required the highest supersaturation at almost every temperature when the soot particle was treated with approximately one monolayer of sulfuric acid. However, the critical supersaturation required for ice formation was much lower when BC particles were treated with a multilayer equivalent coverage of sulfuric acid. Mohler et al. (2005) investigated ice nucleation of soot particles generated from a Graphite Spark Generator (GSG) at 185–240 K, and found that internal mixtures of soot and sulfuric acid required higher supersaturation than that of uncoated soot to nucleate ice. The uncoated lamp black soot used by DeMott et al. (1999) and the GSG soot used by Mohler et al. (2005) have very different ice nucleation properties, with the uncoated GSG soot being a much more efficient ice nuclei (Kärcher et al., 2007). Friedman et al. (2011) found no heterogeneous ice nucleation below water saturation above their experimental detection limit (which was about 0.01–0.1 % of the soot particle concentration, or about $10\,l^{-1}$) for both coated and uncoated soot particles generated from a mini-CAST Real Soot Generator at 253 K and 243 K. Above water saturation, ice nucleation could have occurred for both coated and uncoated soot but could not be distinguished from droplet formation. Crawford et al. (2011) examined nucleation of ice at 210–235 K for sulfuric acid coated soot particles generated from a CAST propane burner with various amounts of organic content. They found that uncoated soot particles with 30 % organic mass content freeze before water saturation, and those with 80 % and 90 % organic mass content are inactive or freeze at water saturation respectively. After coating by sulfuric acid, they all nucleated ice close to the

ACPD
12, 19987–20006, 2012

homogeneous freezing conditions of sulphuric acid. These studies all lead to different conclusions about the effect of adding a soluble coating to soot. One possible reason for the differences in nucleation is the differences in the properties of the bare soot particles, for example, the organic content, porosity, surface area, etc. The amounts of sulfuric acid coating were not quantified in most of these laboratory studies. This hinders the comparability among different laboratory studies, and also the applicability of the results to modeling studies. Furthermore, the results are usually expressed as a freezing onset condition (for example, the ice supersaturation required for activation of 0.1 % or 1 % the aerosols), which are not directly comparable to the input needed in a numerical model after a typical time step of 30 min. Nevertheless, these studies demonstrated that the addition of a soluble coating can alter the ice nucleation ability of soot particles, which most model studies of aerosol indirect effects (AIE) do not explicitly consider (e.g., Yun and Penner, 2012; Lohmann and Hoose, 2009; Storelvmo et al., 2011). Here we adopt recent laboratory studies from Popovicheva et al. (2008, 2010, 2011) and Koehler et al. (2009), which provide a link between sulfuric acid coating, hygroscopicity, and ice nucleation efficiencies, and develop a method of differentiating hydrophobic, hydrophilic, and hygroscopic particles and their ice nucleation in models.

Popovicheva et al. (2008, 2010) suggested that the hygroscopicity of soot could be quantified by the amount of water film extended over the soot surface at relative humidity $< 80\,\%$. Hydrophobic soot never forms a film, while hydrophilic soot does develops a film. Hygroscopic soot develops several layers of water uptake. Popovicheva et al. (2011) identified the threshold amount of sulfate coating needed to transform hydrophobic to hydrophilic to hygroscopic soot as 1 monolayer and 3 monolayers. These thresholds are used here. Koehler et al. (2009) performed a series of experiments to link soot hygroscopicity to its IN ability, based on Popovicheva et al. (2008, 2010). The frozen fractions of hydrophobic, hydrophilic, and hygroscopic soot were measured at various conditions, which are also used here to differentiate their freezing abilities.

We implemented a 3-ffBC/OM (3-hydrophobic, hydrophilic and hygroscopic) soot scheme in place of a single category scheme (1-ffBC/OM) (Wang et al., 2009). We

ACPD
12, 19987–20006, 2012

present the hydrophobic, hydrophilic and hygroscopic ffBC/OM aerosol fields, as well as the cloud water field and radiative forcing from the original and the new scheme. Finally, an updated total anthropogenic forcing is presented with the new 3-ffBC/OM scheme.

2 Methods

The 3-ffBC/OM scheme was implemented into the CAM-IMPACT coupled aerosol transport model and general circulation model (Wang and Penner, 2010), as well as an offline radiation model. The coupled model (inline simulation) provides the aerosol fields and meteorology fields for the offline model, and is used to calculate the total anthropogenic forcing. The offline model reads the aerosol and meteorology fields and examines the cloud water fields and mixed-phase cloud anthropogenic forcing without involving feedbacks to the cloud fields from changes in aerosols.

2.1 Models

The University of Michigan IMPACT aerosol model has a detailed description of the interaction of sulfate with non-sulfate aerosols through condensation, coagulation, as well as aqueous formation of sulfuric acid in cloud droplets (e.g., Wang et al., 2009). Although BC and OM are treated as distinct species in the model, they are assumed to be internally mixed (Liu et al., 2005). The NCAR CAM3 model was updated to include a two-moment microphysics scheme for cloud liquid and ice (Wang and Penner, 2010). In mixed-phase clouds, the Phillips et al. (2008) parameterization (PH08) of deposition/condensation/immersion freezing was implemented (Yun and Penner, 2012). The contact freezing parameterization is that of Young (1974), with the contact ice nuclei concentration fitted to that recommended by Young (1974).

The offline radiation model of Chen and Penner (2005) was extended to include mixed-phase clouds. The ice nucleation scheme in mixed-phase clouds is the same

ACPD
12, 19987–20006, 2012

as that in the CAM-IMPACT model (Yun and Penner, 2012). The Bergeron-Findeisen process (the conversion of liquid to ice) was also implemented in the offline radiation model, due to its importance to radiative forcing (Storelvmo et al., 2008b). However, no further processing of ice particles takes place (no sedimentation, coagulation, or precipitation formation). Therefore, the anthropogenic forcing in mixed-phase clouds calculated from the offline radiation model is similar to the 1st indirect effect of aerosols, with the added effect of the Bergeron-Findeisen process.

2.2 3-ffBC/OM scheme

The differentiation between hydrophobic, hydrophilic, and hygroscopic ffBC/OM aerosols is based on the number of monolayers of sulfuric acid coating. Freshly emitted ffBC/OM particles are assumed to be hydrophobic. After each time step, the number of monolayers of sulfate coating (n_{coat}) is calculated and compared with threshold values. If $n_{coat} < 1$, the particle remains hydrophobic. If $1 \leq n_{coat} < 3$, the particle is moved to the hydrophilic category. If $n_{coat} \geq 3$, the particle becomes hygroscopic. The size distributions of the three ffBC/OM species prior to coating by sulfate (and water) are assumed fixed (see Penner et al., 1998). The accommodation coefficient for the, condensation of sulfuric acid on hydrophobic and hydrophilic particles is set to 0.018 (Zhang et al., 2005), while that for hygroscopic particles is 0.65, similar to sulfuric acid surfaces (Pöschl et al., 1998).

The PH08 parameterization was modified to treat the nucleation of ice in mixed-phase clouds by the 3-ffBC/OM categories. Ice nucleation was measured at −40 °C as well as at a colder temperature (−51.5 °C or −57 °C) in Koehler et al. (2009). Due to the coexistence of liquid and ice, water saturation is assumed in mixed-phase clouds in our model. Therefore, we use the frozen fraction measured at −40 °C at water saturation to adjust the PH08 parameterization in mixed-phase clouds. For hydrophobic and hydrophilic soot, we use the data for the 200 nm particles because this size is close to the volume mean diameter of the BC/OM particles in our model which is 180 nm. There are only data for polydisperse particles at −40 °C for hygroscopic soot. However, the frozen

ACPD
12, 19987–20006, 2012

fractions of the polydisperse particles and 250 nm particles are similar at −57 °C. So we assumed that differences between the size distribution between the polydisperse particles and our soot particles would not have a large impact on the freezing properties of hygroscopic particles. The frozen fraction of hydrophobic, hydrophilic, and hygroscopic soot measured at −40 °C and at water saturation is 0.03 %, 2 %, and 3 %, respectively, while that predicted by PH08 for the same conditions is 0.2 %. Therefore, we increased the PH08 frozen fraction by a factor of 10 for hydrophilic ffBC/OM, and reduced it by a factor of 0.15 for hydrophobic ffBC/OM. In doing so, we preserve the temperature dependence specified in PH08. Freezing for hygroscopic particles followed the "Koop" line for homogeneous freezing of pure dissolved solute at −40 °C for a short distance near water saturation. However, the frozen fraction slightly above water saturation was far smaller than that predicted by a homogeneous freezing mechanism. Therefore, we made two assumptions to treat the freezing of hygroscopic particles at higher temperatures. The first is that these particles freeze homogeneously, so we exclude them as a heterogeneous IN. This is similar to the observation of internally mixed propane burner soot by Crawford et al. (2011). The second is that they freeze heterogeneously, and we scale the frozen fraction of PH08 by a factor of 15. This is similar to the observation of multi-layer coated lamp black soot by DeMott et al. (1999). The contact freezing treatment was kept the same as in the 1-ffBC/OM scheme, since we want to examine the effect of treating soot ice nucleation using the results of Koehler et al. (2009), whose measurement includes deposition/condensation/immersion freezing but no contact freezing. Contact freezing in our model is represented by the Young (1974) parameterization fitted to the observation of total number of contact ice nuclei measured by Blanchard (1957) (see Yun and Penner, 2012). This treatment makes the contribution from contact freezing to total ice nucleation very small (on the order of 1 %).

ACPD
12, 19987–20006, 2012

2.3 Experiment set-up

Table 1 shows the three offline simulations. In the 1BC simulation, the original PH08 scheme is used and the sum of hydrophobic, hydrophilic, and hygroscopic ffBC/OM is treated as one species. For each configuration, the model is run twice with Present-Day (PD) and Pre-Industrial (PI) aerosol fields. PI aerosol fields are only applied to ice nucleation in mixed-phase clouds. The in-line model is run using the 3BC_noSCO scheme with PD and PI emission files described in Penner et al. (2009). Aerosol direct effects as well as effects on warm-phase and cirrus clouds are included in the in-line model.

3 Results

3.1 Aerosol fields for hydrophobic, hydrophilic, and hygroscopic ffBC/OM

Figure 1 shows the PD horizontal distribution of column integrated hydrophobic, hydrophilic and hygroscopic ffBC/OM. Hydrophobic ffBC/OM is confined mainly to regions near emissions. Hydrophilic ffBC/OM is transported farther than hydrophobic ffBC/OM. Hygroscopic ffBC/OM is even more wide spread. The majority of the ffBC/OM particles are hygroscopic, contributing 69.93 % to the total ffBC/OM burden. Hydrophilic and hydrophobic ffBC/OM particles contribute 17.64 % and 12.43 %, respectively. The lifetime of the ffBC/OM particles increases with hygroscopicity from 0.45 to 0.95 to 4.55 days.

Figure 2 shows the change in the hydrophobic, hydrophilic, and hygroscopic ffBC/OM number concentrations from PI to PD due to anthropogenic emissions. Concentrations increase in most places due to higher PD emissions. However, the concentration of hydrophobic ffBC/OM is smaller for the PD in most places of the Northern Hemisphere (NH) (Fig. 2a), and the concentration of hydrophilic ffBC/OM is smaller for PD at NH high latitudes (Fig. 2b). This is because sulfate emissions increase significantly in the PD in the industrial regions in the NH and more readily coat the surface of the ffBC/OM

ACPD
12, 19987–20006, 2012

particles. Therefore, the ffBC/OM particles become hygroscopic more easily and are less likely to remain hydrophilic and even less likely to remain hydrophobic.

3.2 Comparison of mixed-phase cloud water field and radiative forcing

Figure 3 shows the grid-mean ice number concentration (N_i) change from PI to PD in mixed-phase clouds using the offline model. There is a larger increase in N_i in the NH than in the Southern Hemisphere (SH) for all three experiments. The 1BC case shows increases of order $1\,l^{-1}$ throughout the mid-troposphere north of 30° N, while the 3BC_noSCO case shows decreases north of 60° N, caused by the decrease of hydrophilic ffBC/OM (Fig. 2b). The 3BC_SCO case shows much larger increases that also extend to the SH, due to the enhanced effect of hygroscopic ffBC/OM. In general, N_i increases from PI to PD predicted by the 3-ffBC/OM scheme is very different from that predicted by the 1-ffBC/OM scheme. However, the sign of the change depends strongly on the freezing ability of hygroscopic ffBC/OM. When hygroscopic ffBC/OM acts as a heterogeneous IN in mixed-phase clouds, there is a larger increase in N_i; when hygroscopic ffBC/OM does not, there is a smaller overall increase.

An increase in N_i causes a net conversion of liquid to ice in mixed-phase clouds, as a result of the Bergeron-Findeisen process. Figure 4 shows the change in the liquid water mass mixing ratio in all 3 schemes from PI to PD. Liquid cloud mass mixing ratio decreases at most latitudes except north of 60° N in the 3BC_noSCO scheme. The decrease is largest in the 3BC_SCO case and smallest in the 3BC-noSCO case, consistent with the changes in N_i.

Table 2 shows the anthropogenic forcing in mixed-phase clouds from the three cases. Two aspects contribute to the anthropogenic ffBC/OM forcing. The first is the decrease of ice effective radius associated with the increase of N_i (Fig. 3). Smaller ice effective radius leads to more reflected solar radiation and less long-wave transmission, reducing the net incoming short-wave radiation as well as the net outgoing long-wave radiation at the Top-of-the-Atmosphere (TOA). Therefore, the anthropogenic Short-wave (SW) forcing from this effect is negative, and the Long-wave (LW) forcing is positive. The

ACPD
12, 19987–20006, 2012

second aspect is the decrease of liquid water mass mixing ratio (Fig. 4). This results in a smaller liquid water path in the present-day, and therefore a reduced short-wave reflectivity and increased long-wave transmissivity. The result of this change is a positive SW forcing and a negative LW forcing. As shown in Table 2, the second effect dominates the sign of the SW and LW forcings.

The treatment of ffBC/OM with different freezing properties results in significant changes to the offline mixed-phase cloud forcing. When hygroscopic ffBC/OM particles are excluded as IN, there is a 35 % decrease in the net anthropogenic forcing compared to the 1BC case. When hygroscopic ffBC/OM particles are included, there is an increase by a factor of 6, due to the large liquid water change in the 3BC_SCO case. The two treatments for hygroscopic soot particles lead to a net offline mixed-phase anthropogenic forcing that varies by almost a factor of 10, from 0.111 to 1.059 $W m^{-2}$.

The total anthropogenic forcing (including sulfate) using the 3BC scheme with the coupled model shows a positive Net CF of 0.06 $W m^{-2}$, which is opposite to the sign of the result of this model in Storelvmo et al. (2012) (−0.8 $W m^{-2}$, manuscript in preparation). The reason is two fold. The first is that both homogenous and heterogeneous freezing are included in cirrus clouds here, whereas only homogeneous freezing is included in Storelvmo et al. (2012). Including heterogeneous freezing in cirrus clouds suppresses homogeneous freezing, results in decreased cirrus ice number concentrations in the PD, and produces a positive SWCF change from PI to PD, if the decrease in cirrus cloud fraction is not very large. The second is that the anthropogenic emission increase is larger for the emission files used here (described in Penner et al., 2009) than in the emission files used in Storelvmo et al. (2012) (which are based on Dentener et al., 2006). With larger aerosol concentrations in PD, there is a larger blocking of the aerosol direct effect (ADE) by clouds which produces a positive PD-PI SWCF, and this effect is enhanced by a larger increase in emissions. The net whole-sky forcing is the same as the CF in the offline simulations because the aerosol and meteorology fields are fixed and no direct effect is included. That for the inline model, however, has all effects including warm cloud, cirrus cloud, and direct effects and is −2.45 $W m^{-2}$.

ACPD
12, 19987–20006, 2012

However, this number would be smaller if hygroscopic soot particles were allowed to act as IN in mixed phase clouds in the in-line simulation.

4 Discussion

Anthropogenic aerosol emissions are thought to produce negative forcing through their indirect effect on warm clouds. This could counteract the warming effect of greenhouse gases and thus has important implications for predicting climate change. However, there are large uncertainties associated with their effects in mixed-phase clouds, which hinders our ability to fully determine the effects of aerosols on climate. Our results show that the net effect of anthropogenic aerosols on mixed-phase clouds is a warming. This warming effect comes from the decrease of optical depth due to the Bergeron-Findeisen process. To estimate the importance of mixed-phase cloud forcing relative to other clouds, we removed the effect of ADE ($0.67\,W\,m^{-2}$ estimated using the offline radiation model) from the inline anthropogenic SWCF to estimate the forcing from only the AIE ($1.61\,W\,m^{-2}$). As a result, the SW forcing in mixed-phase clouds contributes $7.33 \sim 68.7\,\%$ of the anthropogenic SW forcing in all clouds, and the LW forcing contributes $0.32 \sim 2.12\,\%$ (Table 2). The magnitude of the mixed-phase cloud forcing is very sensitive to whether the effect of hygroscopicity is considered, and how it is considered. It is larger when hygroscopic particles are included as IN due to the larger fraction of soot particles acting as ice nuclei. More laboratory experiments are needed to fully determine the freezing properties of hygroscopic ffBC/OM at mixed-phase cloud temperatures to reduce the range of uncertainty.

Acknowledgements. J. E. P. and Y. Y. are grateful for support from US CRDF/NFS, NSF ATM 0609836, and DOE DE-FG02-97-ER62370 and FG0201 ER63248. O. P. appreciates the financial support from projects CRDF-RFBR 2949 and RFBR 12-05-00395_a. R. Chen helped with model set up. L. Xu provided useful suggestions. We are grateful for computer time provided by the NCAR Computational Information Systems Laboratory.

ACPD
12, 19987–20006, 2012

References

Blanchard, D. C.: The supercooling, freezing and melting of giant waterdrops at terminal velocity in air, in: Artificial Simulation of Rain, London, Pergamon Press, 233–249, 1957.

Chen, Y. and Penner, J. E.: Uncertainty analysis for estimates of the first indirect aerosol effect, Atmos. Chem. Phys., 5, 2935–2948, doi:10.5194/acp-5-2935-2005, 2005.

Cozic, J., Mertes, S., Verheggen, B., Cziczo, D. J., Gallavardin, S. J., Walter, S., Baltensperger, U., and Weingartner, E.: Black carbon enrichment in atmospheric ice particle residuals observed in lower tropospheric mixed phase clouds, J. Geophys. Res.-Atmos., 113, D15209, doi:10.1029/2007JD009266, 2008.

Crawford, I., Möhler, O., Schnaiter, M., Saathoff, H., Liu, D., McMeeking, G., Linke, C., Flynn, M., Bower, K. N., Connolly, P. J., Gallagher, M. W., and Coe, H.: Studies of propane flame soot acting as heterogeneous ice nuclei in conjunction with single particle soot photometer measurements, Atmos. Chem. Phys., 11, 9549–9561, doi:10.5194/acp-11-9549-2011, 2011.

DeMott, P. J., Chen, Y., Kreidenweis, S. M., Rogers, D. C., and Sherman, D. E.: Ice formation by black carbon particles, Geophys. Res. Lett., 26, 2429–2432, doi:10.1029/1999GL900580, 1999.

Friedman, B., Kulkarni, G., Beranek, J., Zelenyuk, A., Thornton, J. A., and Cziczo, D. J.: Ice nucleation and droplet formation by bare and coated soot particles, J. Geophys. Res.-Atmos., 116, 17203–17203, doi:10.1029/2011JD015999, 2011.

Kärcher, B., Möhler, O., DeMott, P. J., Pechtl, S., and Yu, F.: Insights into the role of soot aerosols in cirrus cloud formation, Atmos. Chem. Phys., 7, 4203–4227, doi:10.5194/acp-7-4203-2007, 2007.

Koehler, K. A., DeMott, P. J., Kreidenweis, S. M., Popovicheva, O. B., Petters, M. D., Carrico, C. M., Kireeva, E. D., Khokhlova, T. D., and Shonija, N. K.: Cloud condensation nuclei and ice nucleation activity of hydrophobic and hydrophilic soot particles, Phys. Chem. Chem. Phys., 11, 7906–7920, 2009.

Liu, X. H., Penner, J. E., and Herzog, M.: Global modeling of aerosol dynamics: model description, evaluation, and interactions between sulfate and nonsulfate aerosols, J. Geophys. Res.-Atmos., 110, D18206, doi:10.1029/2004JD005674, 2005.

Lohmann, U. and Hoose, C.: Sensitivity studies of different aerosol indirect effects in mixed-phase clouds, Atmos. Chem. Phys., 9, 8917–8934, doi:10.5194/acp-9-8917-2009, 2009.

ACPD
12, 19987–20006, 2012

Mohler, O., Buttner, S., Linke, C., Schnaiter, M., Saathoff, H., Stetzer, O., Wagner, R., Karmer, M., Mangold, A., Ebert, V., and Schurath, U.: Effect of sulfuric acid coating on heterogeneous ice nucleation by soot aerosol particles, J. Geophys. Res.-Atmos., 110, D11210, doi:10.1029/2004JD005169, 2005.

Penner, J. E., Chuang, C. C., and Grant, K.: Climate forcing by carbonaceous and sulfate aerosols, Clim. Dynam., 14, 839–851, 1998.

Penner, J. E., Chen, Y., Wang, M., and Liu, X.: Possible influence of anthropogenic aerosols on cirrus clouds and anthropogenic forcing, Atmos. Chem. Phys., 9, 879–896, doi:10.5194/acp-9-879-2009, 2009.

Phillips, V. T. J., DeMott, P. J., and Andronache, C.: An empirical parameterization of heterogeneous ice nucleation for multiple chemical species of aerosol, J. Atmos. Sci., 65, 2757–2783, 2008.

Pöschl, U., Canagaratna, M., Jayne, J. T., Molina, L. T., Worsnop, D. R., Kolb, C. E., and Molina, M. J.: Mass accommodation coefficient of H_2SO_4 vapor on aqueous sulfuric acid surfaces and gaseous diffusion coefficient of H_2SO_4 in N_2/H_2O, J. Phys. Chem. A, 102, 10082–10089, 1998.

Popovicheva, O. B., Persiantseva, N. M., Tishkova, V., Shonija, N. K., and Zubareva, N. A.: Quantification of water uptake by soot particles, Environ. Res. Lett., 3, 025009, doi:10.1088/1748-9326/3/2/025009, 2008.

Popovicheva, O. B., Kireeva, E. D., Timofeev, M. A., Shonija, N. K., and Mogil'nikov, V. P.: Carbonaceous aerosols of aviation and shipping emissions, Izv. Atmos. Ocean. Phy., 46, 339–346, 2010.

Popovicheva, O. B., Persiantseva, N. M., Kireeva, E. D., Khokhlova, T. D., and Shonija, N. K.: Quantification of the hygroscopic effect of soot aging in the atmosphere: laboratory simulations, J. Phys. Chem. A, 115, 298–306, 2011.

Storelvmo, T., Kristjansson, J. E., and Lohmann, U.: Aerosol influence on mixed-phase clouds in CAM-Oslo, J. Atmos. Sci., 65, 3214–3230, 2008a.

Storelvmo, T., Kristjansson, J. E., Lohmann, U., Iversen, T., Kirkevag, A., and Seland, O.: Modeling of the Wegener-Bergeron-Findeisen process – implications for aerosol indirect effects, Environ. Res. Lett., 3, 45001–45001, 2008b.

Storelvmo, T., Hoose, C., and Eriksson, P.: Global modeling of mixed-phase clouds: the albedo and lifetime effects of aerosols, J. Geophys. Res.-Atmos., 116, 5207–5207, doi:10.1029/2010JD014724, 2011.

ACPD
12, 19987–20006, 2012

Wang, M. and Penner, J. E.: Cirrus clouds in a global climate model with a statistical cirrus cloud scheme, Atmos. Chem. Phys., 10, 5449–5474, doi:10.5194/acp-10-5449-2010, 2010.
Wang, M. H., Penner, J. E., and Liu, X. H.: Coupled IMPACT aerosol and NCAR CAM3 model: evaluation of predicted aerosol number and size distribution, J. Geophys. Res.-Atmos., 114, D06302, doi:10.1029/2008JD010459, 2009.
Young, K. C.: Numerical-simulation of wintertime, orographic precipitation 1. Description of model microphysics and numerical techniques, J. Atmos. Sci., 31, 1735–1748, 1974.
Yun, Y. and Penner, J. E.: Global model comparison of heterogeneous ice nucleation parameterizations in mixed phase clouds, J. Geophys. Res.-Atmos., 117, D07203, doi:10.1029/2011JD016506, 2012.
Zhang, D. and Zhang, R. Y.: Laboratory investigation of heterogeneous interaction of sulfuric acid with soot, Environ. Sci. Technol., 39, 5722–5728, 2005.
Zhang, R. Y., Khalizov, A. F., Pagels, J., Zhang, D., Xue, H. X., and McMurry, P. H.: Variability in morphology, hygroscopicity, and optical properties of soot aerosols during atmospheric processing, P. Natl. Acad. Sci. USA, 105, 10291–10296, 2008.

ACPD
12, 19987–20006, 2012

Table 1. Offline simulations.

Schemes	Description
1BC	1-ffBC/OM scheme
3BC_SCO	3-ffBC/OM scheme and hygroscopic particles as heterogeneous ice nuclei
3BC_noSCO	3-ffBC/OM scheme and no hygroscopic particles as heterogeneous ice nuclei

ACPD
12, 19987–20006, 2012

Table 2. Annual average anthropogenic cloud forcings (CF) and whole-sky forcings ($W\,m^{-2}$). Off-line forcings are for mixed-phase clouds, while inline forcings include all effects: warm, mixed-phase, and cirrus clouds and direct effects.

	SWCF	LWCF	Net CF	Net Whole-Sky
1BC	0.188	−0.0173	0.171	0.171
3BC_SCO	1.106	−0.0470	1.059	1.059
3BC_noSCO	0.118	−0.007	0.111	0.111
3BC_noSCO (inline)	2.28	−2.22	0.06	−2.45

ACPD
12, 19987–20006, 2012

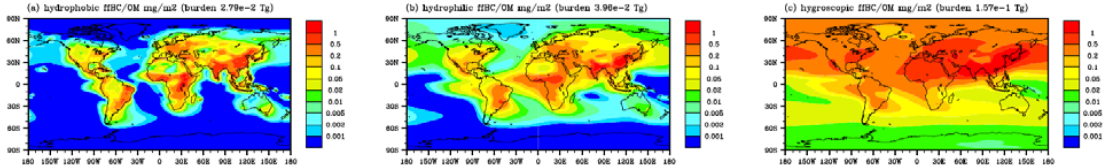

Fig. 1. PD annual average horizontal distribution of column integrated hydrophobic **(a)**, hydrophilic **(b)**, and hygroscopic **(c)** ffBC/OM (mg m^{-2}).

ACPD
12, 19987–20006, 2012

The effects of hygroscopicity of fossil fuel combustion

Y. Yun et al.

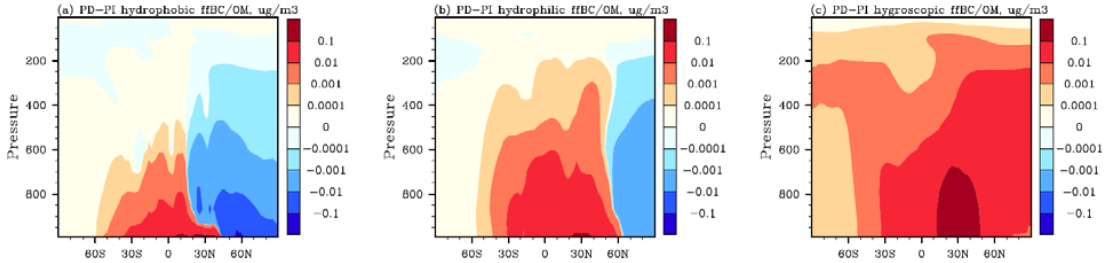

Fig. 2. PD-PI annual average changes of hydrophobic **(a)**, hydrophilic **(b)**, and hygroscopic **(c)** ffBC/OM ($\mu g\,m^{-3}$).

ACPD
12, 19987–20006, 2012

The effects of hygroscopicity of fossil fuel combustion

Y. Yun et al.

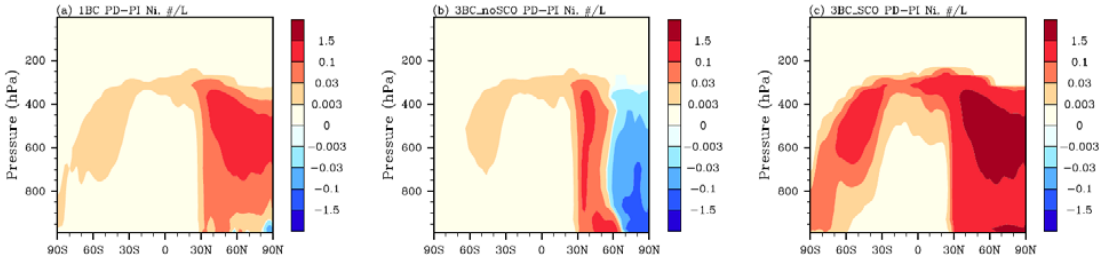

Fig. 3. PD-PI annual average changes of grid-mean ice number concentration in mixed-phase clouds from 1BC **(a)**, 3BC_noSCO **(b)** and 3BC_SCO **(c)** simulations ($\#\,l^{-1}$).

ACPD
12, 19987–20006, 2012

The effects of hygroscopicity of fossil fuel combustion

Y. Yun et al.

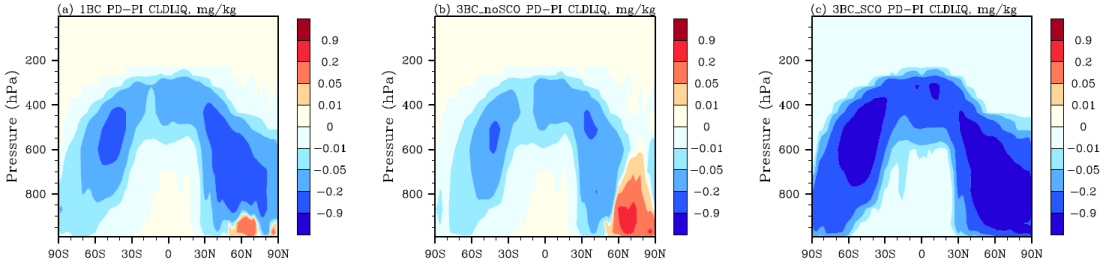

Fig. 4. PD-PI annual average changes of grid-mean liquid water mass mixing ratio (CLDLIQ) in mixed-phase clouds from 1BC **(a)**, 3BC_noSCO **(b)** and 3BC_SCO **(c)** simulations (mg kg^{-1}).

ACPD
12, 19987–20006, 2012

The effects of hygroscopicity of fossil fuel combustion

Y. Yun et al.